Evolution of the Magnetic Structure in $CeCu_{5.5}Au_{0.5}$ under Pressure towards Quantum Criticality

A. Hamann,[1,2] O. Stockert,[3] V. Fritsch,[2] K. Grube,[1] A. Schneidewind,[4] and H. v. Löhneysen[1,2]

[1]*Institut für Festkörperphysik, Karlsruhe Institute of Technology (KIT), D-76131 Karlsruhe, Germany*
[2]*Physikalisches Institut, Karlsruhe Institute of Technology (KIT), D-76131 Karlsruhe, Germany*
[3]*Max-Planck-Institut für Chemische Physik fester Stoffe, D-01187 Dresden, Germany*
[4]*Gemeinsame Forschergruppe Helmholtz-Zentrum Berlin—TU Dresden, D-85747 Garching, Germany*

(Received 14 November 2012; published 28 February 2013)

In the prototypical heavy-fermion system $CeCu_{6-x}Au_x$, a magnetic quantum critical point can be tuned by Au concentration x, hydrostatic pressure p, or magnetic field B. A striking equivalence of the tuning behavior with x or p had been found with respect to thermodynamic and transport properties. By means of elastic neutron scattering on single crystalline $CeCu_{5.5}Au_{0.5}$, we demonstrate this $x - p$ equivalence on a microscopic level by showing that the magnetic ordering wave vector $\mathbf{q}_m$ can be tuned accordingly. At ambient pressure,$CeCu_{5.5}Au_{0.5}$ orders at $\mathbf{q}_m \approx (0.590\,0)$. Upon applying $p = 4.1$ kbar, $\mathbf{q}_m \approx (0.61\,0\,0.21)$ is found corresponding to $CeCu_{5.6}Au_{0.4}$ at ambient pressure. The transition seems to occur in a first-order fashion and to be governed by slight changes in the nesting properties of the Fermi surface.

DOI: 10.1103/PhysRevLett.110.096404 PACS numbers: 71.27.+a, 75.20.Hr, 75.25.−j, 75.30.Mb

Fermi-liquid (FL) theory is the cornerstone to understanding the physics of metals with interacting electrons [1]. Assuming a one-to-one correspondence between their electronic excitations (called quasiparticles) and those of the noninteracting electron gas, FL theory successfully describes the excitations and their properties in a vast number of different materials including heavy-fermion systems with very large, effective masses m^*. $CeCu_6$, a prototypical heavy-fermion compound, is, at low temperatures T, rather well-described by FL theory: A FL hallmark is the T^2 dependence of the electrical resistivity between 40 and 200 mK [2] that is characteristic of dominant quasiparticle-quasiparticle scattering [3]. The huge Sommerfeld coefficient $\gamma = 1.6$ J/mol K^2 of the specific heat C and the strongly enhanced magnetic susceptibility χ [2,4], both depending only weakly on T, reflect the very large effective mass m^* of the quasiparticles, directly observed in de Haas–van Alphen experiments [5].

Substituting Cu by isoelectronic Au introduces long-range antiferromagnetism (AF) in the alloying series $CeCu_{6-x}Au_x$ for $x > x_c \approx 0.1$, with a Néel temperature $T_N(x)$ increasing linearly up to $x = 1$ (cf. Fig. 1). In the vicinity of the quantum critical point (QCP) at $x = x_c$, i.e., at the magnetic instability where $T_N(x) = 0$, significant deviations from FL behavior, nicknamed non-FL (NFL) behavior, have been observed in macroscopic such as thermodynamic and transport properties [6,7]. Some of the most notable NFL anomalies are the linear T dependence of the resistivity, $\Delta\rho \propto T$, and the logarithmic divergence of the Sommerfeld coefficient with decreasing T, $C(T)/T \propto -\ln T$. The magnetic ground state can be tuned not only by Au concentration x but also—for samples with $x > x_c$—by applying hydrostatic pressure p. Pressure reverses the increase in unit-cell volume upon Au doping and hence, reduces T_N of magnetically ordered $CeCu_{6-x}Au_x$ with $x > 0.1$ [8]. Adjusting p appropriately even drives T_N to zero resulting in a p-tuned QCP for $x > x_c$ [6,9]. Remarkably, the NFL behavior at the respective p-tuned QCP has been found to be identical to the x-tuned QCP at $x = x_c$ and ambient p, indicating a striking equivalence of the tuning behavior with x or p [6,7].

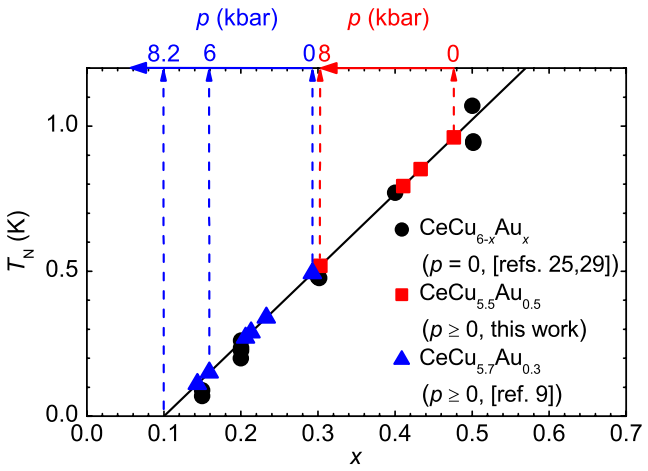

FIG. 1 (color online). Data shown in black: The Néel temperature T_N of $CeCu_{6-x}Au_x$ at ambient pressure $p = 0$ vs Au concentration x as determined from specific heat and magnetic susceptibility [25,29]. The line is a linear fit taking into account additional data (not shown) up to $x = 1$. Data shown in blue: T_N of $CeCu_{5.7}Au_{0.3}$ ($x = 0.3$) at different p as determined from specific heat [9]. Data shown in red: T_N of $CeCu_{5.5}Au_{0.5}$ ($x = 0.5$) at different p as determined from neutron scattering data and explained in the following (cf. Fig. 3). In order to compare the effects of Au doping and hydrostatic pressure, T_N was mapped onto x by virtue of the linear fit.

This fact is particularly remarkable since it suggests that disorder (introduced by the random occupation of the Cu(2) site in $CeCu_6$ by Au for $0 < x < 1$) does not have a decisive effect on the NFL behavior at the respective QCP. Structural disorder might lead to a distribution of single-ion Kondo temperatures T_K, so-called Kondo disorder. The superposition of local Fermi liquids with different T_K can then lead to apparent NFL behavior [10,11]. For $CeCu_{5.9}Au_{0.1}$, no indication of short-range Kondo disorder has been found in NMR and μSR experiments, as opposed to $UCu_{5-x}Pd_x$, where NFL behavior was also reported [12]. The NFL behavior can, therefore, be related inequivocally to the QCP. However, the observed features disagree with the standard Hertz-Millis-Moriya (HMM) model [13–15] while the anomalous $C/T \sim \ln T$ and $\Delta\rho \sim T$ dependencies can be accounted for by two-dimensional (2D) magnetic fluctuations [16] which indeed have been identified via inelastic neutron scattering (INS) [17], the ω/T scaling observed in INS [18] is clearly incompatible with the HMM model. This dichotomy has prompted alternative theoretical scenarios [19], the most elaborate one suggesting that the Kondo effect (which in $CeCu_{6-x}Au_x$ is the origin of the heavy masses) breaks down at a "local" QCP [20]. This scenario has been adopted to explain the unusual properties of $YbRh_2Si_2$ close to a QCP which can be tuned by small magnetic fields [21,22].

For magnetically ordered $CeCu_{6-x}Au_x$ with $x = 0.2$ on the other hand, the thermodynamic and transport properties when using a magnetic field to tune the QCP are found to follow the 3D HMM model [23] which was later corroborated by INS yielding $\omega/T^{1.5}$ scaling [24]. These findings are in marked contrast to the macroscopic properties at the concentration- and pressure-tuned QCP mentioned above. Hence, it is of primary importance to investigate if the concentration—pressure ($x - p$) equivalence holds on a microscopic level, e.g., by virtue of the magnetic ordering wave vector $\mathbf{q}_m := (q_h\, q_k\, q_l)$.

Previous neutron-scattering experiments on $CeCu_{6-x}Au_x$ single crystals at ambient pressure [17,23,25] revealed an abrupt change of $\mathbf{q}_m$: Upon increasing, x, $q_l(x)$ first decreases slowly and then abruptly drops to zero between $x = 0.4$ and $x = 0.5$ as shown in Fig. 4 below, while $T_N(x)$ varies linearly (cf. Fig. 1). This unusual behavior needs clarification, even more so since $T_N(x)$ varies linearly between $x = 0.1$ and 1 [7]. Therefore, we investigated the p dependence of $\mathbf{q}_m$ in $CeCu_{5.5}Au_{0.5}$ using elastic neutron scattering to determine if $\mathbf{q}_m$ corresponding to $x = 0.4$ [25] can be recovered by applying pressure. This should also shed light on the microscopic properties upon approaching the QCP.

The neutron-scattering measurements were performed on the cold triple-axis spectrometer PANDA operated at the FRM-II reactor in Garching. A new single crystal of $CeCu_{5.5}Au_{0.5}$ was grown with the Czochralski method [26]. The starting materials were weighted in the desired nominal composition (Ce [27], Au 99.99%, Cu 99.999%) and the crystal was pulled out of a tungsten crucible under argon atmosphere ($p = 1$ bar). X-ray powder diffraction patterns showed the sample to be single phase. Atomic absorption spectroscopy confirmed a homogeneous Au concentration $x \approx 0.5$ throughout the whole sample. The actual Au concentration x as determined by its T_N and the linear $T_N(x)$ relation is $x = 0.48$, i.e., slightly below $x = 0.5$. The crystal was cut by spark erosion into a cylindrical shape ($\varnothing \approx 5$ mm, $l \approx 10$ mm, axis along the orthorhombic b direction, mass $m \approx 1.7$ g) in order to fit into the Cu:Be clamped pressure cell, together with a piece of Pb whose superconducting transition $T_c(p)$ measured inductively served as a pressure gauge (uncertainty about 0.1 kbar). Fluorinert FC 72 was used as pressure medium. In order to reduce the background generated by scattering from the pressure cell, a Cd shielding was wrapped around leaving open only the sample space. All data were taken in the elastic condition ($k_i = k_f = 1.5$ Å^{-1}) to avoid inelastic contributions. The use of a dilution refrigerator enabled cooling the sample to below 100 mK (with beam on). The scattering plane was spanned by the reciprocal [1 0 0] and [0 0 1] axes. We focused on scans over the magnetic Bragg peak in the $\mathbf{G} = (2\,0\,0)$ Brillouin zone due to the large structure factor and the low background there. The instrument was operated with doubly focusing monochromator and analyzer, a Be filter in the incident beam, and open collimation.

Figures 2(a)–2(d) show the p dependence of neutron intensity of $CeCu_{5.5}Au_{0.5}$ on a grid in the reciprocal (h 0 l) plane. Measurements at ambient p [Fig. 2(a), performed with the sample in the pressure cell] reveal a strong magnetic Bragg peak at the incommensurate position $\mathbf{Q} := (h\ k\ l) = (1.412\ 0\ -0.005)$ in excellent agreement with previous results [28] where $\mathbf{Q} = (1.41\,0\,0)$ was found. The small deviation of l from zero is due to slight misalignments of the spectrometer and the sample orientation resulting in an uncertainty of about 0.004 r.l.u. The comparatively small background (< 6% of the peak intensity) varies quadratically along (h 0 0) and linearly along (0 0 l) and is taken into account in any fit mentioned in the following. Upon applying $p = 3.6$ kbar, the position of the Bragg peak significantly changes to $\mathbf{Q} = (1.402\,0\,0.194)$ resuming almost the same l that had been found for $CeCu_{5.6}Au_{0.4}$ at ambient pressure [25]. This indicates that by pressure tuning the sample towards the QCP, not only the thermodynamic and transport data [6] but also the magnetic ordering wave vector of lower doping x are recovered. On the other hand, increasing p to 4.1 kbar and even 8 kbar does not significantly change the Bragg position [$\mathbf{Q} = (1.405\,0\,0.195)$ at $p = 8$ kbar]. Previous measurements revealed the p dependence of T_N of $CeCu_{6-x}Au_x$ with $x = 0.2$, $x = 0.3$, and $x = 0.5$ [9,29,30]. Judging from these results a pressure

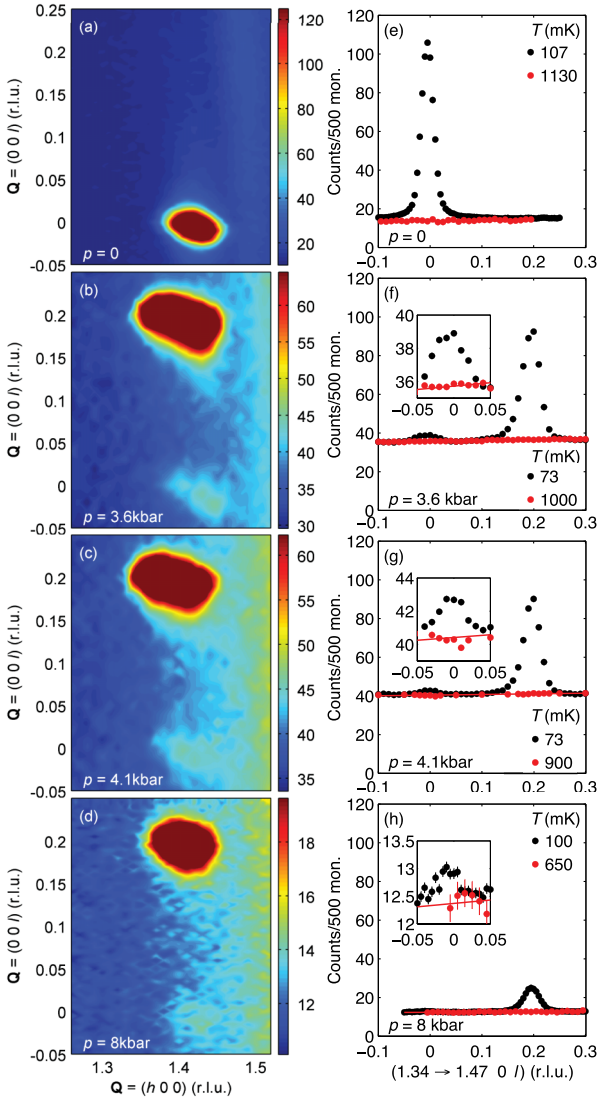

FIG. 2 (color online). (a–d) Pressure p dependence [zero (a) to 8 kbar (d)] of neutron intensity (counts/500 mon., see color code) at base temperature ($T = 73$–107 mK) revealing magnetic Bragg peaks of $CeCu_{5.5}Au_{0.5}$ in the reciprocal $(h\,0\,l)$ plane. $\mathbf{Q} = \mathbf{q}_m + \mathbf{G}$ is shown with $\mathbf{G} = (2\,0\,0)$. The color scale is adapted to reveal weak remnant peaks around $l \approx 0$ in (b, c, d); thus, strong peaks look less well-defined than they are. (e–h) Intensity along $(0\,0\,l)$ summed along $(h\,0\,0)$ for $1.34 \leq h \leq 1.47$ at T below (black) and above (red) $T_N(p)$. Solid lines are fits to data above $T_N(p)$. Insets show the range $-0.05 \leq l \leq 0.05$ on an expanded scale.

of ~8 kbar should have the same effect as decreasing the Au content by about $\Delta x = 0.2$. Consequently, a small but noticeable increase of l upon increasing p from 3.6 to 8 kbar would be expected, in analogy to corresponding data towards lower doping, where $\mathbf{Q} = (1.38\,0\,0.25)$ was found for $x = 0.3$ [25]. Moreover, a small remnant peak at the position corresponding to ambient pressure ($l \approx 0$) is present at all $p > 0$ shown in Fig. 2. We checked the magnetic origin of this feature by heating the sample above $T_N(p)$ where it disappears completely just as the strong magnetic Bragg peak does [cf. Figs. 2(e)–2(h)]. This behavior is indicative of a first-order phase transition with a partition of the sample into different domains, most of which reveal magnetic order within the $(h\ 0\ l)$ plane but some along $(h\,0\,0)$, too. This first-order transition between two magnetically ordered states at low pressure with the occurrence of phase separation over the studied pressure range ($p \lesssim 8$ kbar) is to be contrasted to the complete disappearance of magnetic order at the QCP expected at $p \approx 16$ kbar for $CeCu_{5.5}Au_{0.5}$ (cf. Fig. 1) and being second order in nature.

The detailed T dependence of the intensity of the strong magnetic Bragg peak at all p is depicted in Fig. 3. Surprisingly, data at $p = 3.6$ kbar and 4.1 kbar coincide at low T whereas, zero intensity is reached at significantly different T_N, proving the actual difference in p. This effect may be due to an intensity shift from the weak remnant peak at $l \approx 0$ to the strong peak at $l \approx 0.2$ with increasing p. As a result, the intensity for $T \rightarrow 0$ may accidentally happen to be the same at both p. In fact, panels (f) and (g) of Fig. 2 are indicative of such behavior. However, additional data at even higher p, eventually showing that the small remnant peak disappears before the strong one does, would be needed to support this scenario. Describing the T dependence of the normalized magnetic intensity $I_{magn.}/I_{(200)}$ phenomenologically by

$$I(T) = I_0\left(\frac{T_N - T}{T_N}\right)^y \qquad (1)$$

over the entire temperature range below T_N yields the Néel temperatures $T_N(p)$ and intensities $I_0(p)$ extrapolated to $T = 0$. Data obtained at ambient p are properly described

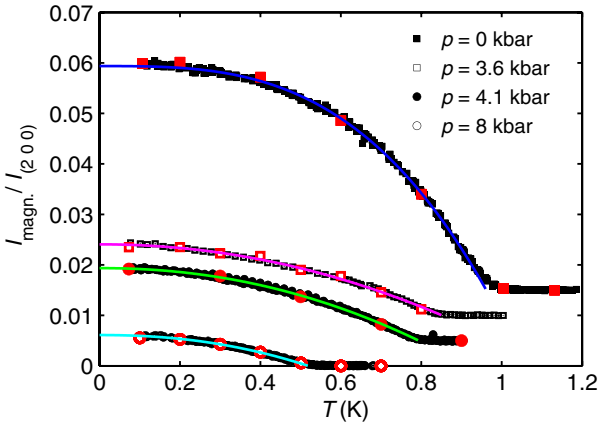

FIG. 3 (color online). T dependence of the magnetic Bragg peak intensity normalized to the nuclear (2 0 0) Bragg peak. Data shown in black were measured at the peak position extracted from a 2D Gaussian fit to data shown in Figs. 2(a)–2(d). Red symbols reveal the amplitude extracted from 2D fitting several scans over the Bragg peak along $(h\,0\,0)$ and $(0\,0\,l)$ at each T and are in agreement with black symbols. Lines depict fits of Eq. (1) to the data. For clarity, data and fits for different pressures are shifted vertically by 0.005 with respect to each other.

by an exponent $y = 3.08(2)$ which is slightly larger than the previously found $y = 2.5$ [28]. The extraction of $T_N = 962(1)$ mK at $p = 0$ indicates that the actual Au content of our sample is indeed very close to $x = 0.5$, where $T_N = 1.022$ K is expected according to the linear fit shown in Fig. 1. Furthermore, the reduction of $T_N(p)$ to 794(1) mK and 519(1) mK at $p = 4.1$ kbar and 8 kbar, respectively, corroborates that the sample was tuned very close to $x = 0.4$ and $x = 0.3$ behavior, where the linear fit gives $T_N = 767$ mK and $T_N = 511$ mK. Even more, the exponent $y = 2.20(4)$ for $p = 8$ kbar is in good agreement with $y = 2$ found for $x = 0.3$ at ambient pressure [31]. Note that close to T_N all $I(T)$ data signal a linear dependence with $y = 1$, corresponding to mean-field behavior with $\beta = y/2 = 1/2$.

In order to determine $\mathbf{q}_m$ of $CeCu_{5.5}Au_{0.5}$ most reliably, we pinpointed the positions of related Bragg peaks not only in the vicinity of the nuclear (2 0 0) Bragg peak (cf. Fig. 2) but in several other Brillouin zones as well (not shown). Resulting average values of $\mathbf{q}_m$ are presented in Fig. 4 in comparison to corresponding $CeCu_{6-x}Au_x$ alloys at ambient p. This comparison demonstrates that applying $p = 3.6$ and 4.1 kbar recovers q_h and q_l of corresponding

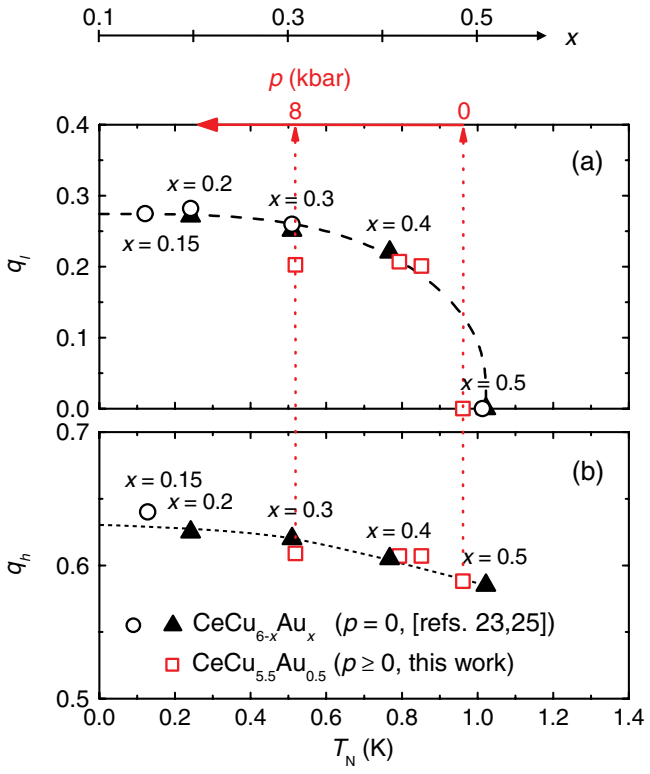

FIG. 4 (color online). Components q_l (a) and q_h (b) of the magnetic ordering wave vector $\mathbf{q}_m = (q_h\, 0\, q_l)$ vs T_N of several systems $CeCu_{6-x}Au_x$. The p dependence at $x = 0.5$ (red) is shown in comparison to the x-dependence at $p = 0$ (black, previous work [23,25]). Data are mapped onto $T_N(x)$ by virtue of the linear fit shown in Fig. 1. Dashed lines are guides to the eye.

x at $p = 0$, corroborating the assumed $x - p$ equivalence. However, no significant difference in $\mathbf{q}_m$ is observed between $p = 3.6$ and 8 kbar as opposed to a significant increase in q_h and q_l towards smaller x (black symbols). Despite the lack of data towards even higher p, this behavior is indicative of an intrinsic discrepancy between tuning with x and p at least on a quantitative basis. On the other hand, subtle differences are somewhat expected from the different impact of the respective tuning parameter on the form of the unit cell [29]: Pressure contracts all lattice parameters simultaneously as opposed to the substitution of Cu by Au which affects them in an anisotropic fashion. Therefore, instead of the volume of the unit cell, T_N being the most direct measure of competing energy scales was chosen as the parameter allowing the most reasonable comparison between systems with different x at different p. The abrupt change of $\mathbf{q}_m$ around $T_N \approx 1$ K being universal in respective x- or p-tuned $CeCu_{6-x}Au_x$ points towards a phase transition of the first order. This scenario is supported by the double-peak structure (Fig. 2) that is revealed in $CeCu_{5.5}Au_{0.5}$ at $p \geq 3.6$ kbar (i.e., $T_N \leq 851$ mK). It might be due to a Fermi surface providing two nesting vectors at $p \geq 3.6$ kbar of which the corresponding energy levels are populated very differently with a clear preference of $q_l \approx 0.2$. Another feature of $CeCu_{6-x}Au_x$ hints at a first-order transition as well: At $x_c = 0.1$, dynamic correlations appear revealing a rod-like structure in $\mathbf{Q}$ space [17]. They can be regarded as a precursor of incipient ordering at slightly larger x, because corresponding Bragg peaks are located *on* these rods. In contrast, magnetic Bragg peaks for $x \geq 0.4$ are located *away* to the rods, ruling out any direct relation of the quantum critical fluctuations with magnetic order at $x = 0.5$.

To conclude, elastic neutron scattering was performed on $CeCu_{5.5}Au_{0.5}$ under hydrostatic pressure. Our experiments reveal that the magnetic ordering wave vector $\mathbf{q}_m$ in $CeCu_{6-x}Au_x$ can be tuned by applying pressure and resumes values of correspondingly lower doping levels x at ambient conditions. The equivalence of the tuning behavior with concentration x and pressure p on a microscopic and macroscopic level and even far away from the QCP at $x = 0.5$ suggests that disorder (whose effect should be most pronounced for $x = 0.5$) cannot have a decisive effect on the approach to quantum criticality in the system $CeCu_{6-x}Au_x$. The transition from alloys ordering along $(h\ 0\ 0)$ to those where q_l assumes a finite value, seems to happen in a first-order fashion. However, subtle differences on a quantitative basis between both tuning behaviors need further attention and should be addressed in future investigations. Ultimately, the goal must be to tune antiferromagnetically ordered $CeCu_{5.5}Au_{0.5}$ to quantum criticality by pressure and investigate the spin fluctuations there in order to gain more insight into the mechanisms that drive the quantum phase transition.

We gratefully acknowledge the hospitality at FRM-II, especially the supply of liquid helium to perform the neutron scattering experiments. In particular, we thank D. Etzold for his excellent technical support at the PANDA spectrometer. This work is supported by the Deutsche Forschungsgemeinschaft through Research Unit FOR 960 ''Quantum Phase Transitions''.

[1] L. Landau, Sov. Phys. JETP **3**, 920 (1957).
[2] Y. Onuki, Y. Shimizu, and T. Komatsubara, J. Phys. Soc. Jpn. **54**, 304 (1985).
[3] A. Amato, D. Jaccard, J. Flouquet, F. Lapierre, J. L. Tholence, R. A. Fisher, S. E. Lacy, J. A. Olsen, and N. E. Phillips, J. Low Temp. Phys. **68**, 371 (1987).
[4] H. R. Ott, H. Rudigier, Z. Fisk, J. O. Willis, and G. R. Stewart, Solid State Commun. **53**, 235 (1985).
[5] S. Chapman, M. Hunt, P. Meeson, P. H. P. Reinders, M. Springford, and M. Norman, J. Phys. Condens. Matter **2**, 8123 (1990).
[6] H. v. Löhneysen, J. Phys. Condens. Matter **8**, 9689 (1996).
[7] H. v. Löhneysen, A. Rosch, M. Vojta, and P. Wölfle, Rev. Mod. Phys. **79**, 1015 (2007).
[8] A. Germann and H. v. Löhneysen, Europhys. Lett. **9**, 367 (1989).
[9] B. Bogenberger and H. v. Löhneysen, Phys. Rev. Lett. **74**, 1016 (1995).
[10] R. N. Bhatt and D. S. Fisher, Phys. Rev. Lett. **68**, 3072 (1992).
[11] E. Miranda and V. Dobrosavljević, Rep. Prog. Phys. **68**, 2337 (2005).
[12] O. O. Bernal, D. E. MacLaughlin, A. Amato, R. Feyerherm, F. N. Gygax, A. Schenck, R. H. Heffner, L. P. Le, G. J. Nieuwenhuys, and B. Andraka *et al.*, Phys. Rev. B **54**, 13000 (1996).
[13] J. A. Hertz, Phys. Rev. B **14**, 1165 (1976).
[14] A. J. Millis, Phys. Rev. B **48**, 7183 (1993).
[15] T. Moriya and T. Takimoko, J. Phys. Soc. Jpn. **64**, 960 (1995).
[16] A. Rosch, A. Schröder, O. Stockert, and H. v. Löhneysen, Phys. Rev. Lett. **79**, 159 (1997).
[17] O. Stockert, H. v. Löhneysen, A. Rosch, N. Pyka, and M. Loewenhaupt, Phys. Rev. Lett. **80**, 5627 (1998).
[18] A. Schröder, G. Aeppli, R. Coldea, M. Adams, O. Stockert, H. v. Löhneysen, E. Bucher, R. Ramazashvili, and P. Coleman, Nature (London) **407**, 351 (2000).
[19] P. Coleman, C. Pépin, Q. Si, and R. Ramazashvili, J. Phys. Condens. Matter **13**, R723 (2001).
[20] Q. Si, S. Rabello, K. Ingersent, and J. L. Smith, Nature (London) **413**, 804 (2001).
[21] J. Custers, P. Gegenwart, H. Wilhelm, K. Neumaier, Y. Tokiwa, O. Trovarelli, C. Geibel, F. Steglich, C. Pépin, and P. Coleman, Nature (London) **424**, 524 (2003).
[22] Q. Si and F. Steglich, Science **329**, 1161 (2010).
[23] H. v. Löhneysen, A. Neubert, T. Pietrus, A. Schröder, O. Stockert, U. Tutsch, M. Loewenhaupt, A. Rosch, and P. Wölfle, Eur. Phys. J. B **5**, 447 (1998).
[24] O. Stockert, M. Enderle, and H. v. Löhneysen, Phys. Rev. Lett. **99**, 237203 (2007).
[25] H. Okumura, K. Kakurai, Y. Yoshida, Y. Onuki, and Y. Endoh, J. Magn. Magn. Mater. **177–181**, 405 (1998).
[26] *Handbook of Crystal Growth*, edited by D. T. J. Hurle (Elsevier, Amsterdam, 1994), Vol. 2.
[27] Rare-earth metals acquired from Materials Preparation Center, Ames Laboratory, US DOE Basic Energy Sciences, Ames, IA, USA, http://www.mpc.ameslab.gov.
[28] A. Schröder, J. W. Lynn, R. W. Erwin, M. Loewenhaupt, and H. v. Löhneysen, Physica (Amsterdam) **199B–200B**, 47 (1994).
[29] T. Pietrus, B. Bogenberger, S. Mock, M. Sieck, and H. v. Löhneysen, Physica (Amsterdam) **206B–207B**, 317 (1995).
[30] M. Sieck, F. Huster, and H. v. Löhneysen, Physica (Amsterdam) **230B–232B**, 583 (1997).
[31] O. Stockert, Ph.D. thesis, Physikalisches Institut, Universität Karlsruhe, Cuvillier Verlag Göttingen, 1999.